

# On the Performance of Dual-Antenna Repeater Assisted Bi-Static MIMO ISAC

Anubhab Chowdhury and Erik G. Larsson, *Fellow, IEEE*

**Abstract**—This paper presents a framework for target detection and downlink data transmission in a repeater-assisted bi-static integrated sensing and communication system. A repeater is an active scatterer that retransmits incoming signals with a complex gain almost instantaneously, thereby enhancing sensing performance by amplifying the echoes reflected by the targets. The same mechanism can also improve downlink communication by mitigating coverage holes. However, the repeater introduces noise and increases interference at the sensing receiver, while also amplifying the interference from target detection signals at the downlink users. The proposed framework accounts for these sensing-communication trade-offs and demonstrates the potential benefits achievable through a carefully designed precoder at the transmitting base station. In particular, our finding is that a higher value of probability of detection can be attained with considerably lower target radar-cross-section variance by deploying repeaters in the target hot-spot areas.

**Index Terms**—Repeater, Integrated sensing and communication, Massive MIMO, GLRT

## I. INTRODUCTION

**R**EPEATERS (also known as full-duplex relays) are active scatterers, capable of receiving and retransmitting signals instantly with amplification [1]. They can be deployed on a large scale to enhance coverage for multiple-input multiple-output (MIMO) wireless systems [1]–[6]. Reference [3] demonstrated that repeaters can procure a spectral-efficiency (SE) similar to that of distributed MIMO, while obviating the front-haul signalling overhead. Furthermore, [7] indicated that repeaters can outperform reconfigurable intelligent surface (RIS)-assisted systems, with the additional advantage of repeaters being band/frequency selective. The attractive implementation aspects of repeaters have led to their inclusion in the 5G NR standards since 3rd Generation Partnership Project (3GPP) Release 18 [8].

On parallel avenue, integrated sensing and communication (ISAC) offers efficient spectral and hardware utilization, and is actively being pushed forward as part of 3GPP Release 19, a 5G-advanced/pre-6G initiative [9]. A detailed survey of ISAC is beyond the scope of this paper; readers can refer to [10]–[12] and references therein, and specifically for bi-static ISAC, [13], [14]. The authors in [15] considered repeater-assisted *mono-static* ISAC,<sup>1</sup> where the repeater was

The authors are with the Department of Electrical Engineering (ISY), Linköping University, 58183 Linköping, Sweden. Emails: {anuch87, erik.g.larsson}@liu.se

This work was supported in part by the Knut and Alice Wallenberg (KAW) foundation, Excellence Center at Linköping-Lund in Information Technology (ELLIT), and the Swedish Research Council (VR).

<sup>1</sup>In a mono-static setting, the base station (BS) is required to be full-duplex, which in turn incurs additional signal processing and hardware overhead for self-interference cancellation.

used to improve the coverage for downlink communication users. In contrast to [15], we investigate the feasibility of *bi-static* ISAC in the presence of a repeater (specifically, a dual-antenna repeater as in [3, Fig. 2]), focusing on the effects of the repeater on the performance of both target detection and downlink communication.

In bi-static ISAC, one of the BSs transmits precoded downlink data and a dedicated signal for target detection. The other BS performs joint clutter-channel and radar cross-section (RCS) estimation, as well as target detection, using the reflected echoes. In this setting, *ideally*, a repeater can enhance the overall ISAC performance in two ways: (a) by amplifying the echo reflected from the target, which in turn can improve the detection performance; (b) by removing coverage-holes for the downlink users.

However, the repeater also amplifies communication-to-sensing and sensing-to-communication interference. Specifically, the amplified sensing signal can incur increased interference for the communication users. Contrarily, for sensing, should the amplified downlink signals (directly via the repeater) overwhelm the reflected amplified echo of the target, detection performance at the sensing receiver can severely degrade. To this end, this paper investigates these tradeoffs and discusses the *choices of precoders* at the transmit BS that can mitigate this interference while retaining the ISAC performance improvement due to the repeater. Moreover, the *developed generalized likelihood ratio test (GLRT) framework* is agnostic of the channel models and applicable to diverse propagation conditions among the repeater, BS, and users.

## II. SYSTEM MODEL

We consider a bi-static ISAC system where the transmit BS, with  $N_t$  antennas, beamforms a precoded sensing signal towards a target hot-spot area while simultaneously serving  $K$  downlink single-antenna users. The system also contains a dual-antenna repeater. The receiver BS, with  $N_t$  antennas, performs target detection based on the reflected echoes from the target, also via the repeater. The system model from the communication point of view is illustrated in Fig. 1a and the sensing point of view in Fig. 1b. The system entails several desired and interference channels, whose definitions are:

- $\mathbf{f}_n \in \mathbb{C}^{N_t}$ : downlink channel from the transmit BS to the  $n$ th user.
- $h_n \in \mathbb{C}$ : channel from the transmit antenna of the repeater to the receive antenna of the  $n$ th user.
- $\mathbf{a}_t \in \mathbb{C}^{N_t}$ : the channel from the transmitter to the target.
- $\mathbf{b}_t \in \mathbb{C}^{N_t}$ : the channel from the transmitter to the repeater.
- $\mathbf{a}_r \in \mathbb{C}^{N_t}$ : the channel from the target to the receive BS.

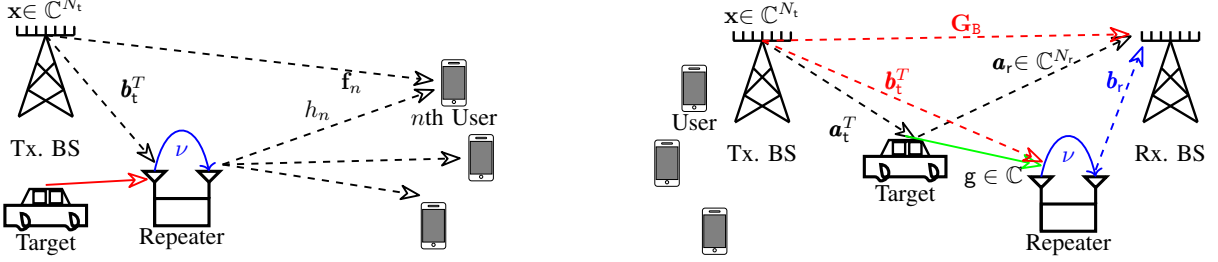


**Fig. 1:** System model: communication and sensing with a repeater, and its implications to both. Interference links are indicated by red arrows.

- $\mathbf{b}_r \in \mathbb{C}^{N_r}$ : the channel from the repeater to the receive BS.
- $g \in \mathbb{C}$ : the channel from the target to the repeater.
- $\mathbf{G}_B \in \mathbb{C}^{N_r \times N_t}$ : the channel from the transmit to receive BS. Also, let  $\hat{\mathbf{G}}_B$  and  $\tilde{\mathbf{G}}_B$  be the estimate and estimation error of this direct link channel between the BSs.
- $\mathbf{C} \in \mathbb{C}^{N_r \times N_t}$ : the composite clutter channel. Specifically, the clutter channel consisting of the LoS and NLoS paths caused by permanent obstacles can be measured beforehand and canceled [16]. The unknown part corresponds to the NLoS paths caused by temporary obstacles, which are encased in  $\mathbf{C}$ .

Apart from the clutter channel, we assume perfect channel state information (CSI) at the receiver for target detection as a necessary first step to understand the overall system performance with an intuitive and tractable formulation.<sup>2</sup> Further, let  $\nu \in \mathbb{C}$  be the repeater amplification factor. The target is characterized by the associated RCS, denoted by  $\alpha$ , which follows  $\alpha \sim \mathcal{CN}(0, \sigma_T^2)$ ,  $\sigma_T^2$  being the RCS variance. The RCS is unknown at the receiver and needs to be estimated. Finally, we adopt a model wherein target detection is performed in a given hotspot, and a larger area can be covered by sending sensing signals to such hotspot areas serially [16].

### III. SIGNALLING SCHEME

Let  $\mathbf{x}[\tau]$  be the precoded downlink transmit signal, transmitted at  $\tau$ th slot, which can be written as:<sup>3</sup>

$$\mathbf{x}[\tau] = \sqrt{\rho} \left\{ \sum_{n=1}^K \sqrt{\pi_n} \mathbf{p}_n s_n[\tau] + \sqrt{\pi_T} \mathbf{p}_T s_T[\tau] \right\}, \quad \tau \in [\tau_L], \quad (1)$$

where,  $\rho$  is the total transmit power at the BS,  $\pi_n$  and  $\pi_T$  denote the fraction of the total power allocated to the  $n$ th downlink user and for sensing, respectively. Also,  $\mathbf{p}_n$  and  $\mathbf{p}_T$  are the corresponding unit-normalized precoding vectors for the  $n$ th downlink user and the target. Similarly,  $s_n \in \mathbb{C}$  and  $s_T \in \mathbb{C}$  are unit-energy, statistically independent symbols.

<sup>2</sup>The composite channel via the target is  $\alpha \mathbf{a}_r \mathbf{a}_t^T$ . We assume only  $\mathbf{a}_r \mathbf{a}_t^T$  to be known, as the BS beamforms to a specific sensing zone whose associated angle of arrival (AoA) and angle of departure (AoD) are pre-calibrated. However,  $\alpha$  is unknown and will be estimated as a part of the GLRT later.

<sup>3</sup>All subsequent analysis is for an arbitrary subcarrier of the underlying orthogonal frequency division multiplexing (OFDM) waveform (or any monochromatic signal with a prefix to remove time-dispersion), without explicitly showing the subcarrier index, i.e., before IFFT and after FFT on the transmitter and the receiver sides; with cyclic-prefix length being larger than the maximum delay spread.

Also,  $\mathbb{E} [\|\mathbf{x}[\tau]\|_2^2] \leq \rho$ , satisfying the total transmit power budget. Finally,  $\tau_L$  is the total duration over which sensing signals are transmitted, which can also be a coherence block. Given this, we can write the input-output receive ( $y_R^I$ ) and transmit ( $y_R^0$ ) signals at the repeater terminals as:

$$y_R^I[\tau] = \alpha g \{ \mathbf{a}_t^T \mathbf{x}[\tau] \} + \mathbf{b}_t^T \mathbf{x}[\tau], \quad (2a)$$

$$y_R^0[\tau] = \nu (y_R^I[\tau] + w_R[\tau]), \quad (2b)$$

where  $w_R[\tau] \sim \mathcal{CN}(0, \sigma_R^2)$  is the additive white Gaussian noise (AWGN) at the repeater.

1) *Sensing with repeater*: The signal received at the BS can be expressed as:

$$\mathbf{y}_{BS}[\tau] = \alpha \mathbf{a}_r \mathbf{a}_t^T \mathbf{x}[\tau] + \mathbf{b}_r y_R^0[\tau] + \mathbf{G}_B \mathbf{x}[\tau] + \mathbf{C} \mathbf{x}[\tau] + \mathbf{w}_B[\tau], \quad (3)$$

where  $\mathbf{w}_B[\tau] \sim \mathcal{CN}(\mathbf{0}_{N_r}, \sigma_{BS}^2 \mathbf{I}_{N_r})$  is the AWGN at the BS. Knowledge of the transmitted signal  $\mathbf{x}[\tau]$  can be made available at the receiver BS via back-haul links and thus be treated as pilot symbols. Then, the receive BS can subtract  $\hat{\mathbf{G}}_B \mathbf{x}[\tau]$  from  $\mathbf{y}_{BS}$  to reduce inter-BS interference. After this, substituting for  $y_R^0$ , the desired signal for the target detection and associated interference terms become:

$$\mathbf{y}_{BS}[\tau] = \mathbf{r}[\tau] \alpha + \dot{\mathbf{C}} \mathbf{x}[\tau] + \dot{\mathbf{w}}_B[\tau], \quad (4)$$

where the equivalent sensing channel  $\mathbf{R}[\tau]$ , equivalent clutter channel  $\dot{\mathbf{C}}$ , and the overall sensing noise  $\dot{\mathbf{w}}_B[\tau]$ , respectively, can be written as:

$$\mathbf{r}[\tau] = (\mathbf{a}_r \mathbf{a}_t^T + \nu g \{ \mathbf{b}_r \mathbf{a}_t^T \}) \mathbf{x}[\tau], \quad (5a)$$

$$\dot{\mathbf{C}} = \mathbf{C} + \nu \mathbf{b}_r \mathbf{b}_t^T, \quad (5b)$$

$$\dot{\mathbf{w}}_B[\tau] = \hat{\mathbf{G}}_B \mathbf{x}[\tau] + \{\nu w_R[\tau]\} \mathbf{b}_r + \mathbf{w}_B[\tau]. \quad (5c)$$

The direct (amplified) interference due to the repeater, i.e.,  $\{\nu \mathbf{b}_r \mathbf{b}_t^T \mathbf{x}[\tau]\}$ , is incorporated as a part of the clutter. However, the composite channel can be pre-estimated (in LoS, it can even be fully characterized by AoAs and AoDs) to cancel this interference, similar to inter-BS interference.<sup>4</sup> The resulting  $\dot{\mathbf{C}} \approx \mathbf{C}$  encases the effects of environmental scatterers. Later, with (4), we will develop the target detection framework.

<sup>4</sup>This can also be cancelled by choosing the precoder for target  $\left( \mathbf{I}_{N_t} - \frac{1}{\|\mathbf{b}_t\|_2^2} \mathbf{b}_t^* \mathbf{b}_t^T \right) \mathbf{a}_t$ , leading to the direct link interference  $\nu \mathbf{b}_r \mathbf{b}_t^T \mathbf{p}_T = 0$ , where  $\mathbf{p}_T$  is the precoder intended for the target. Although it is not necessary for the subsequent analyses.

2) *Downlink communication with repeater*: For downlink communication analysis, we drop the explicit dependence of index  $\tau$ . The signal received at the  $n$ th downlink user can be expressed as

$$y_{\text{UE}} = \mathbf{f}_n^T \mathbf{x} + h_n \{ \nu(\alpha g\{\mathbf{a}_t^T \mathbf{x}\} + \mathbf{b}_t^T \mathbf{x} + w_{\text{R}}) \} + w_{\text{UE}}, \quad (6)$$

where the second term corresponds to the repeater transmission and  $w_{\text{UE}} \sim \mathcal{CN}(0, \sigma_{\text{UE}}^2)$  is AWGN at the UE. Rearranging (6), we get

$$y_{\text{UE}} = (\mathbf{f}_n^T + \nu h_n \mathbf{b}_t^T) \mathbf{x} + \dot{w}_{\text{UE}}, \quad (7)$$

with  $\dot{w}_{\text{UE}} = (\nu h_n w_{\text{R}} + w_{\text{UE}})$ .

**Remark 1.** Note that the term “ $\nu \alpha h_n g\{\mathbf{a}_t^T \mathbf{x}\}$ ” in (6) can be subsumed in the effective downlink channel of the users, i.e.,  $\{\mathbf{f}_n\}$ ; and is therefore not explicitly shown in (7). This is because the user is agnostic of the presence of the target, and any reflection from it can be treated as from any other environmental scatterers.

Next, based on (4) and (7), we present GLRT-based target detection framework and downlink signal-to-interference-plus-noise ratio (SINR) analysis.

#### IV. RCS ESTIMATION & TARGET DETECTION

Let  $\bar{\mathbf{y}}_{\text{BS}} \triangleq [\mathbf{y}_{\text{BS}}^T[1], \mathbf{y}_{\text{BS}}^T[2], \dots, \mathbf{y}_{\text{BS}}^T[\tau_L]]^T \in \mathbb{C}^{N_r \times \tau_L}$  be the concatenated received signal vector at the BS at the end of the observation window. With this, we can formulate the following binary hypothesis testing framework:

$$\mathcal{H}_0 : \bar{\mathbf{y}}_{\text{BS}} = \bar{\mathbf{c}} + \bar{\mathbf{w}}, \quad (8a)$$

$$\mathcal{H}_1 : \bar{\mathbf{y}}_{\text{BS}} = \bar{\mathbf{r}} + \bar{\mathbf{c}} + \bar{\mathbf{w}}, \quad (8b)$$

where  $\bar{\mathbf{r}}$ ,  $\bar{\mathbf{c}}$ , and  $\bar{\mathbf{w}}$  are the concatenation of  $\mathbf{r}[\tau] \alpha$ ,  $\dot{\mathbf{C}} \mathbf{x}[\tau]$ , and  $\dot{\mathbf{w}}_{\text{B}}[\tau]$ , respectively. The null hypothesis  $\mathcal{H}_0$  represents the case that there is no target in the sensing area, while the alternative hypothesis  $\mathcal{H}_1$  represents the existence of the target. The joint RCS estimation, target-free channel (i.e. clutter) estimation, and the hypothesis testing problem can be written as  $\{\hat{\alpha}, \hat{\mathbf{c}}, \hat{\mathcal{H}}\} = \arg \max_{\{\alpha, \mathbf{c}, \mathcal{H}\}} p(\alpha, \mathbf{c}, \mathcal{H} | \bar{\mathbf{y}}_{\text{BS}})$ , where

$\hat{\mathbf{c}} \triangleq \text{Vec}(\dot{\mathbf{C}})$ <sup>5</sup> and  $p(\alpha, \hat{\mathbf{c}}, \mathcal{H} | \bar{\mathbf{y}}_{\text{BS}})$  is the joint probability density function (pdf) given the received vector  $\bar{\mathbf{y}}_{\text{BS}}$ . Thus, the GLRT can be formulated as  $\mathcal{L} \gtrless \lambda_s$ , where

$$\mathcal{L} = \frac{\max_{\{\alpha, \hat{\mathbf{c}}\}} p(\bar{\mathbf{y}}_{\text{BS}} | \alpha, \hat{\mathbf{c}}, \mathcal{H}_1) p(\alpha | \mathcal{H}_1) p(\hat{\mathbf{c}} | \mathcal{H}_1)}{\max_{\{\hat{\mathbf{c}}\}} p(\bar{\mathbf{y}}_{\text{BS}} | \hat{\mathbf{c}}, \mathcal{H}_0) p(\hat{\mathbf{c}} | \mathcal{H}_0)}, \quad (9)$$

and  $\lambda_s$  is the threshold used by the detector, which is selected to achieve a desired false alarm probability. The final result of the GLRT is given in the following lemma.

**Lemma 1.** Let  $\Sigma_c$  and  $\Sigma_s[\tau]$  denote the covariance of the clutter channel and the overall sensing noise  $\dot{\mathbf{w}}_{\text{B}}[\tau]$  (which are individually zero mean random vectors); and let  $\mathcal{T} \triangleq \ln \mathcal{L}$  be the test statistics, which evaluates to

$$\mathcal{T} = \mathbf{t}_{\mathcal{H}_1}^H \mathbf{Q}_{\mathcal{H}_1}^{-1} \mathbf{t}_{\mathcal{H}_1} - \mathbf{t}_{\mathcal{H}_0}^H \mathbf{Q}_{\mathcal{H}_0}^{-1} \mathbf{t}_{\mathcal{H}_0}, \quad (10)$$

<sup>5</sup>“ $\text{Vec}(\cdot)$ ” stands for vectorization.

where  $\mathbf{t}_{\mathcal{H}_1}$ ,  $\mathbf{t}_{\mathcal{H}_0}$ ,  $\mathbf{Q}_{\mathcal{H}_0}$  are given by

$$\mathbf{t}_{\mathcal{H}_1} = \begin{bmatrix} \sum_{\tau=1}^{\tau_L} \mathbf{r}^H[\tau] \Sigma_s^{-1}[\tau] \mathbf{y}_{\text{BS}}[\tau] \\ \sum_{\tau=1}^{\tau_L} \mathbf{B}^H[\tau] \Sigma_s^{-1}[\tau] \mathbf{y}_{\text{BS}}[\tau] \end{bmatrix}, \quad (11a)$$

$$\mathbf{t}_{\mathcal{H}_0} = \sum_{\tau=1}^{\tau_L} \mathbf{B}^H[\tau] \Sigma_s^{-1}[\tau] \mathbf{y}_{\text{BS}}[\tau], \quad (11b)$$

$$\mathbf{Q}_{\mathcal{H}_0} = \sum_{\tau=1}^{\tau_L} \mathbf{B}^H[\tau] \Sigma_s^{-1}[\tau] \mathbf{B}[\tau] + \Sigma_c^{-1}. \quad (11c)$$

$\mathbf{Q}_{\mathcal{H}_1}$  is given in (13) on the next page, and  $\mathbf{B}[\tau] \triangleq (\mathbf{x}^T[\tau] \otimes \mathbf{I}_{N_r})$ . The resulting test can be evaluated as

$$\hat{\mathcal{H}} = \begin{cases} \mathcal{H}_1, & \text{if } \mathcal{T} \geq \ln \lambda_s', \\ \mathcal{H}_0, & \text{if } \mathcal{T} < \ln \lambda_s'. \end{cases} \quad (12)$$

with  $\lambda_s' (= \pi \lambda_s \sigma_{\text{r}}^2)$  being the detection threshold.

*Proof.* See Appendix A. ■

The complexity of the GLRT is dominated by a matrix inversion of dimension  $(N_t N_r + 1) \times (N_t N_r + 1)$ , and hence is  $\mathcal{O}((N_t N_r + 1)^3)$ . Next, only the parameter remains to be computed in the sensing noise covariance  $\Sigma_s[\tau] = \mathbb{E}[\dot{\mathbf{w}}_{\text{B}}[\tau] \dot{\mathbf{w}}_{\text{B}}^H[\tau]]$ , which is evaluated (treating transmitted symbols as pilots) as

$$\Sigma_s[\tau] = \mathbb{E} \left[ \tilde{\mathbf{G}}_{\text{B}} \mathbf{x}[\tau] \mathbf{x}^H[\tau] \tilde{\mathbf{G}}_{\text{B}}^H \right] + \left\{ |\nu|^2 \sigma_{\text{R}}^2 \right\} \mathbf{b}_{\text{r}} \mathbf{b}_{\text{r}}^H + \sigma_{\text{BS}}^2 \mathbf{I}_{N_r}.$$

Next, if we assume that elements of  $\tilde{\mathbf{G}}_{\text{B}}$  are independent and identically distributed (i.i.d.)  $\mathcal{CN}(0, \zeta^2)$ ,  $\zeta^2$  capturing the power of the residual inter-BS interference [17], then  $\mathbb{E}[\tilde{\mathbf{G}}_{\text{B}} \mathbf{x}[\tau] \mathbf{x}^H[\tau] \tilde{\mathbf{G}}_{\text{B}}^H]$  evaluates to  $\zeta^2 \|\mathbf{x}[\tau]\|_2^2 \mathbf{I}_{N_r}$ , which completes the calculation of  $\Sigma_s[\tau]$ .

**Remark 2.** We note that a noisy repeater can severely degrade the sensing performance, which is captured by  $|\nu|^2 \sigma_{\text{R}}^2$  in the sensing noise covariance. The effect of the amplified downlink signals (directly via the repeater) is implicitly captured in the clutter covariance matrix in (11c).

#### V. DOWNLINK SE ANALYSIS

In downlink, based on (1) and (7), the signal received at the  $n$ th user, with  $\dot{\mathbf{f}}_n \triangleq \mathbf{f}_n + \nu h_n \mathbf{b}_t$ , can be expressed as:

$$y_{\text{UE},n} = \sqrt{\rho} \sqrt{\pi_n} \dot{\mathbf{f}}_n^T \mathbf{p}_n s_n + \sqrt{\rho} \sum_{n'=1, n' \neq n}^K \sqrt{\pi_{n'}} \dot{\mathbf{f}}_n^T \mathbf{p}_{n'} s_{n'} + \sqrt{\rho} \sqrt{\pi_{\text{T}}} \dot{\mathbf{f}}_n^T \mathbf{p}_{\text{T}} s_{\text{T}} + \dot{w}_{\text{UE}}, \quad (14)$$

where the second and the third term correspond to multi-user interference and interference due to a dedicated signal for target detection. The instantaneous SINR at the  $n$ th downlink user can then be written as

$$\text{SINR}_n = \frac{\rho \pi_n |\dot{\mathbf{f}}_n^T \mathbf{p}_n|^2}{\rho \sum_{n'=1, n' \neq n}^K \pi_{n'} |\dot{\mathbf{f}}_n^T \mathbf{p}_{n'}|^2 + \rho \pi_{\text{T}} |\dot{\mathbf{f}}_n^T \mathbf{p}_{\text{T}}|^2 + \mathbb{E}[|\dot{w}_{\text{UE}}|^2]},$$

$$\mathbf{Q}_{\mathcal{H}_1} = \begin{bmatrix} \sum_{\tau=1}^{\tau_L} \mathbf{r}^H[\tau] \mathbf{\Sigma}_s^{-1}[\tau] \mathbf{r}[\tau] + \frac{1}{\sigma_T^2} & \sum_{\tau=1}^{\tau_L} \mathbf{r}^H[\tau] \mathbf{\Sigma}_s^{-1}[\tau] \mathbf{B}[\tau] \\ \left( \sum_{\tau=1}^{\tau_L} \mathbf{r}^H[\tau] \mathbf{\Sigma}_s^{-1}[\tau] \mathbf{B}[\tau] \right)^H & \sum_{\tau=1}^{\tau_L} \mathbf{B}^H[\tau] \mathbf{\Sigma}_s^{-1}[\tau] \mathbf{B}[\tau] + \mathbf{\Sigma}_c^{-1} \end{bmatrix} \in \mathbb{C}^{(N_t N_r + 1) \times (N_t N_r + 1)}. \quad (13)$$

where the noise variance can be computed as

$$\mathbb{E} \left[ |\dot{w}_{\text{UE}}|^2 \right] = |\nu|^2 |h_n|^2 \sigma_R^2 + \sigma_{\text{UE}}^2. \quad (15)$$

Next, for the choice of the precoders, the transmitter can either consider the composite channel  $\{\dot{\mathbf{f}}_n\}$  or be completely agnostic of the repeater and consider  $\{\mathbf{f}_n\}$ . We consider regularized zero-forcing (ZF) precoding scheme for the communication user, in which case  $\mathbf{p}_n$  becomes  $\mathbf{p}_n = \epsilon_n \left( \sum_{n'=1}^K \dot{\mathbf{f}}_{n'} \dot{\mathbf{f}}_{n'}^H + \zeta_{\text{ZF}} \mathbf{I}_{N_t} \right)^{-1} \dot{\mathbf{f}}_n$ , where  $\epsilon_n$  is the normalizer to ensure  $\|\mathbf{p}_n\|_2^2 = 1$  and  $\zeta_{\text{ZF}} > 0$  is a regularizer. For  $\mathbf{p}_T$  we can consider one of the following: *Target centric*: In this case, the transmitter beamforms towards the target, i.e.,  $\mathbf{p}_T = \epsilon_T \dot{\mathbf{f}}_T$ , with  $\dot{\mathbf{f}}_T = \mathbf{a}_T$  and  $\epsilon_T$  is an appropriate normalizer. *Communication centric*: We null the (potentially destructive) interference from the sensing signal to the users by projecting  $\mathbf{p}_T$  onto the nullspace of the subspace spanned by the users' channel vectors. In this case,  $\mathbf{p}_T = \epsilon_T (\mathbf{I}_{N_t} - \mathbf{U} \mathbf{U}^H) \dot{\mathbf{f}}_T$ , where  $\mathbf{U}$  is a unitary matrix formed with the orthonormal columns that span the column space of  $\{\dot{\mathbf{f}}_1, \dot{\mathbf{f}}_2, \dots, \dot{\mathbf{f}}_K\}$ .

## VI. NUMERICAL RESULTS & DISCUSSIONS

In this section, we quantify the effects of a repeater on the overall ISAC performance. The transmit power at the transmit BS is 1 Watt. The path loss for the communication channels is modeled using the 3GPP Urban Microcell model. Each of the BSs is equipped with 8 antennas. The height of the BS, repeaters, and users are 25, 10, and 1.5 meters, respectively, following the models adopted in [1]. The carrier frequency and bandwidth are set to 1.9 GHz and 20 MHz, respectively. At the receive BS, the noise spectral density is  $-174$  dBm/Hz, and the noise figure is 9 dB [12]. The zone area is 500 square meters, with the BSs being in (0, 250) and (450, 250); the sensing zone is (225, 250). The repeater is located at (125, 250). The user locations are randomly generated. The repeater has the same noise power as the BS. The sensing-related parameters follow the Swerling-I model [18] and  $\{\mathbf{a}_t, \mathbf{a}_r\}$  are generated following [16]. For clutter, i.i.d. Gaussian taps are assumed. Other relevant parameters are also mentioned alongside the simulation results. The inter-BS channel and the residual interference is modeled according to [17].

Fig. 2 illustrates the effects of a repeater on the target detection. For this, the repeater is placed within 100 meters of the target hot-spot area, and we consider  $K = 10$  communication users being served by the same BS, whose locations are generated uniformly at random. The slot duration for the GLRT consists of 50 channel uses, i.e.  $\tau = 1, 2, \dots, 50$ . For

simplicity, we assume a Gaussian clutter model. Firstly, we observe that the repeater can substantially improve the target detection performance as it amplifies and forwards the echo from the target and thereby improves the received strength of the echo signal at the BS. Specifically, the repeater-aided system attains a high PoD at a lower value of RCS compared to the traditional bi-static detection scenario. An increase in clutter variance degrades the overall detection performance; however, the repeater-assisted system remains robust to it in contrast with the no repeater case.

In Fig. 3 illustrates the involved trade-offs between the different choices of precoders at the transmit BS. The repeater gain is set to 5 dB above the noise floor. We can readily observe the degradation of the downlink SE for the target-centric precoder, as such a choice adds additional interference to the downlink users due to the dedicated target signals, for both with and without a repeater being present in the system. Communication-centric precoder nullifies that interference. Secondly, we also observe the benefits in the downlink SE due to the repeater.

In Fig. 4, we illustrate the effects of moving the repeater towards the transmitter (varying the  $x$ -axis location) from the target hot-spot area. This experiment reveals that a repeater near the hot-spot area can procure a high probability of detection value even for a lower target RCS. The reflected echo from a repeater, which is also further from the target, suffers severely from pathloss and contributes little to the target detection.

## VII. REMARKS AND OPEN QUESTIONS

This paper presented the initial results and a mathematical framework that facilitates repeater deployment for bi-static ISAC, and reported the benefits that can be obtained by using a repeater in the target hot-spot area. One interesting future study is to incorporate channel estimation within the developed framework and include the time-varying nature of the channels. Furthermore, the impact of multiple repeaters (i.e. swarm-repeaters) in the system, including the effects of interaction between repeaters along with downlink power control, can be interesting to explore. A detailed comparison with other existing technologies, such as RIS, could also be examined as a future study.

## APPENDIX

### A. Proof of Lemma 1

First, let us consider the optimization problem in the numerator of  $\mathcal{L}$  in (9). Recall,  $\mathbf{B}[\tau] \triangleq (\mathbf{x}^T[\tau] \otimes \mathbf{I}_{N_r})$ , then  $\dot{\mathbf{C}}\mathbf{x}[\tau] = \mathbf{B}[\tau]\dot{\mathbf{c}}$ . Further, recall that  $p(\alpha|\mathcal{H}_1)$  and  $p(\dot{\mathbf{c}}|\mathcal{H}_1)$  are respectively  $\mathcal{CN}(0, \sigma_T^2)$  and  $\mathcal{CN}(\mathbf{0}_{N_t N_r}, \mathbf{\Sigma}_c)$ . Then, because

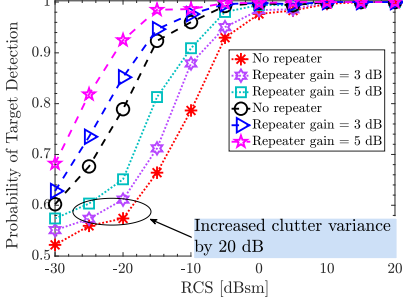


**Fig. 2:** Probability of detection (PoD) versus the target RCS. Here, the repeater gains are measured with respect to the noise floor at the repeater. The threshold for GLRT is adjusted to maintain a probability of false alarm (PoFA) of 0.01.

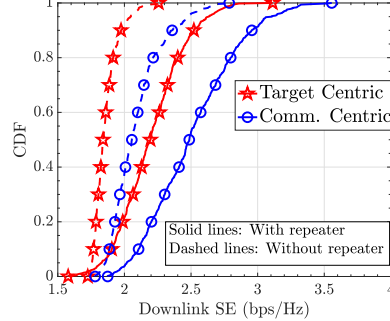


**Fig. 3:** Cumulative distribution function (CDF) of downlink per-user SE with different choices of precoders. Equal power allocation has been employed by the transmit BS.

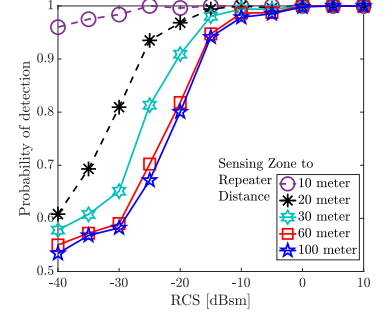


**Fig. 4:** Probability of detection with different repeater locations with respect to the target hotspot area. We assume the clutter variance to be 10 dB below the noise floor and the PoFA is 0.01.

of the temporal independence of the observation vectors, the numerator of  $\mathcal{L}$  is equivalent to the following optimization

$$\begin{aligned} \max_{\{\alpha, \dot{\mathbf{c}}\}} & \left\{ \prod_{\tau=1}^{\tau_L} p(\mathbf{y}_{\text{BS}}[\tau] | \alpha, \dot{\mathbf{c}}, \mathcal{H}_1) \right\} p(\alpha | \mathcal{H}_1) p(\dot{\mathbf{c}} | \mathcal{H}_1) \\ = \max_{\{\alpha, \dot{\mathbf{c}}\}} & \left\{ \prod_{\tau=1}^{\tau_L} p(\dot{\mathbf{w}}_{\text{BS}}[\tau] = \mathbf{y}_{\text{BS}}[\tau] - \mathbf{r}[\tau]\alpha + \mathbf{B}[\tau]\dot{\mathbf{c}} | \alpha, \dot{\mathbf{c}}) \right\} \\ & \times p(\alpha | \mathcal{H}_1) p(\dot{\mathbf{c}} | \mathcal{H}_1) \\ = & C_{\mathcal{H}_1} \exp \left\{ - \min_{\{\alpha, \dot{\mathbf{c}}\}} f(\alpha, \dot{\mathbf{c}}; \mathcal{H}_1) \right\}, \end{aligned}$$

where  $C_{\mathcal{H}_1}$  is a constant and the function  $f(\alpha, \dot{\mathbf{c}}; \mathcal{H}_1)$ , after some algebra, can be expressed as

$$\sum_{\tau=1}^{\tau_L} \mathbf{y}_{\text{BS}}^H[\tau] \mathbf{\Sigma}_s^{-1}[\tau] \mathbf{y}_{\text{BS}} + \mathbf{z}^H \mathbf{Q}_{\mathcal{H}_1} \mathbf{z} - 2\Re\{\mathbf{z}^H \mathbf{t}_{\mathcal{H}_1}\},$$

where  $\mathbf{z} = [\alpha, \dot{\mathbf{c}}^T]^T$  and the positive semi-definite (PSD) matrix  $\mathbf{Q}_{\mathcal{H}_1}$  has the block-structure as shown in (13). Then,  $\mathbf{t}_{\mathcal{H}_1}$  is expressed as shown in (11a). Now, the estimate of  $\mathbf{z}$  obtained from  $f(\alpha, \dot{\mathbf{c}}; \mathcal{H}_1)$  equals to  $\mathbf{Q}_{\mathcal{H}_1}^{-1} \mathbf{t}_{\mathcal{H}_1}$ , resulting

$$-\min_{\{\alpha, \dot{\mathbf{c}}\}} f(\alpha, \dot{\mathbf{c}}; \mathcal{H}_1) = -\sum_{\tau=1}^{\tau_L} \mathbf{y}_{\text{BS}}^H[\tau] \mathbf{\Sigma}_s^{-1}[\tau] \mathbf{y}_{\text{BS}} + \mathbf{t}_{\mathcal{H}_1}^H \mathbf{Q}_{\mathcal{H}_1}^{-1} \mathbf{t}_{\mathcal{H}_1}. \quad (16)$$

Similarly, we can solve the optimization of the denominator of  $\mathcal{L}$ , and show that it evaluates to

$$\begin{aligned} \max_{\{\dot{\mathbf{c}}\}} & p(\bar{\mathbf{y}}_{\text{BS}} | \dot{\mathbf{c}}, \mathcal{H}_0) p(\dot{\mathbf{c}} | \mathcal{H}_0) \\ = & C_{\mathcal{H}_0} \exp \left\{ \mathbf{t}_{\mathcal{H}_0}^H \mathbf{Q}_{\mathcal{H}_0}^{-1} \mathbf{t}_{\mathcal{H}_0} - \sum_{\tau=1}^{\tau_L} \mathbf{y}_{\text{BS}}^H[\tau] \mathbf{\Sigma}_s^{-1}[\tau] \mathbf{y}_{\text{BS}} \right\}, \quad (17) \end{aligned}$$

where  $C_{\mathcal{H}_0}$  is a constant,  $\mathbf{t}_{\mathcal{H}_0}$  and  $\mathbf{Q}_{\mathcal{H}_0}$  are respectively given by (11b) and (11c). Finally, it is easy to show that  $\frac{C_{\mathcal{H}_1}}{C_{\mathcal{H}_0}} = \frac{1}{\pi \sigma_{\tau}^2}$ . Finally, combining (16) and (17), we get the final result.  $\blacksquare$

## REFERENCES

- J. Bai, A. Chowdhury, A. Hansson, and E. G. Larsson, “Repeater swarm-assisted cellular systems: Interaction stability and performance analysis,” *IEEE Trans. Wireless Commun.*, vol. 25, pp. 10 018–10 034, 2026.
- E. G. Larsson, J. Vieira, and P. Frenger, “Reciprocity calibration of dual-antenna repeaters,” *IEEE Wireless Commun. Lett.*, vol. 13, no. 6, pp. 1606–1610, Jun. 2024.
- S. Willhammar *et al.*, “Achieving distributed MIMO performance with repeater-assisted cellular massive MIMO,” *IEEE Commun. Mag.*, vol. 63, no. 3, pp. 114–119, Mar. 2025.
- C.-K. Wen *et al.*, “Shaping a smarter electromagnetic landscape: IAB, NCR, and RIS in 5G standard and future 6G,” *IEEE Commun. Stand. Mag.*, vol. 8, no. 1, pp. 72–78, Mar. 2024.
- K. Dong *et al.*, “Network-controlled repeater aided time-sensitive communications in urban vehicular networks,” *IEEE Wireless Commun. Lett.*, vol. 14, no. 5, pp. 1511–1515, May 2025.
- O. A. Topal, Özlem Tuğfe Demir, E. Björnson, and C. Cavdar, “Fair and energy-efficient activation control mechanisms for repeater-assisted massive MIMO,” 2025. [Online]. Available: <https://arxiv.org/abs/2504.03428>
- M. Åström *et al.*, “RIS in cellular networks – challenges and issues,” 2024. [Online]. Available: <https://arxiv.org/abs/2404.04753>
- 3GPP, “New WID on NR network-controlled repeaters,” 3rd Generation Partnership Project (3GPP), RP 222673, Sep. 2022, TSG RAN meeting no. 97-e. [Online]. Available: [https://www.3gpp.org/ftp/tsg\\_ran/TSG\\_RAN/TSGR\\_97e/Docs/RP-222673.zip](https://www.3gpp.org/ftp/tsg_ran/TSG_RAN/TSGR_97e/Docs/RP-222673.zip)
- A. Kaushik *et al.*, “Toward integrated sensing and communications for 6G: Key enabling technologies, standardization, and challenges,” *IEEE Commun. Standards Mag.*, vol. 8, no. 2, pp. 52–59, June 2024.
- X. Zhu *et al.*, “Enabling intelligent connectivity: A survey of secure ISAC in 6G networks,” *IEEE Commun. Surveys Tuts.*, vol. 27, no. 2, pp. 748–781, Apr. 2025.
- J. A. Zhang *et al.*, “Enabling joint communication and radar sensing in mobile networks—a survey,” *IEEE Commun. Surveys Tuts.*, vol. 24, no. 1, pp. 306–345, Firstquarter 2022.
- M. Elfiatioure *et al.*, “Multiple-target detection in cell-free massive MIMO-assisted ISAC,” *IEEE Trans. Wireless Commun.*, vol. 24, no. 5, pp. 4283–4298, May 2025.
- B. He *et al.*, “Bistatic-enhancement MIMO ISAC: Joint beamforming design in cell-free communication and bistatic radar systems,” *IEEE Trans. Wireless Commun.*, pp. 1–1, 2025.
- X. Shen *et al.*, “Fundamental tradeoff of bistatic ISAC under Gaussian fading channels at finite blocklength,” *IEEE Trans. Inf. Theory*, pp. 1–1, 2025.
- H. Åkesson, D. P. M. Osorio, and E. G. Larsson, “Impact of network-controlled repeaters in integrated sensing and communication systems,” in *Proc. IEEE Eur. Signal Process. Conf.*, Sep. 2025.
- Z. Behdad *et al.*, “Multi-static target detection and power allocation for integrated sensing and communication in cell-free massive MIMO,” *IEEE Trans. Wireless Commun.*, vol. 23, no. 9, pp. 11 580–11 596, Sep. 2024.
- A. Chowdhury and C. R. Murthy, “Half-duplex APs with dynamic TDD versus full-duplex APs in cell-free systems,” *IEEE Trans. Commun.*, vol. 72, no. 7, pp. 3856–3872, Jul. 2024.
- Z. Wei *et al.*, “Integrated sensing and communication channel modeling: A survey,” *IEEE Internet Things J.*, vol. 12, no. 12, pp. 18 850–18 864, Jun. 2025.